B. TECH. PROJECT REPORT

On

ROLE OF MICROSTRUCTURE ON THE NANOINDENTATION RESPONSE OF HARD AND SOFT PZT MATERIALS

BY

HARSHAL SONAGARA

DISCIPLINE OF METALLURGY ENGINEERING AND MATERIALS SCIENCE

INDIAN INSTITUTE OF TECHNOLOGY INDORE

DECEMBER 2019

ROLE OF MICROSTRUCTURE ON THE NANOINDENTATION RESPONSE OF HARD AND SOFT PZT MATERIALS

A PROJECT REPORT

Submitted in partial fulfillment of the requirements for the award of the degrees

of
BACHELOR OF TECHNOLOGY
in
METALLURGY ENGINEERING AND MATERIALS SCIENCE

Submitted by:
HARSHAL SONAGARA

Guided by:
DR. ESWARA PRASAD KORIMILLI,
ASSISTANT PROFESSOR, IIT INDORE

INDIAN INSTITUTE OF TECHNOLOGY INDORE
DECEMBER 2019

CANDIDATE'S DECLARATION

I hereby declare that the project entitled "Role Of Microstructure On The Nanoindentation Response Of Hard And Soft PZT Materials" submitted in partial fulfillment for the award of the degree of Bachelor of Technology in 'Metallurgy Engineering and Materials Science' completed under the supervision of Dr. Eswara Prasad Korimilli, Assistant Professor, Department of Metallurgy Engineering and Materials Science, IIT Indore is an authentic work.

Further, I declare that I have not submitted this work for the award of any other degree elsewhere.

Harshal Sonagara

CERTIFICATE by BTP Guide

It is certified that the above statement made by the student is correct to the best of my knowledge.

Dr. Eswara Prasad Korimilli

Assistant Professor, IIT Indore

PREFACE

This report on “Role Of Microstructure On The Nanoindentation Response Of Hard And Soft PZT Materials” is prepared under the guidance of Dr. Eswara Prasad Korimilli. This report aims to investigate the role of microstructure on the nanomechanical behaviour of piezoceramics. I have tried to the best of my abilities and knowledge to explain the content in a lucid manner.

Harshal Sonagara
B.Tech. IV Year
Discipline of Metallurgy Engineering and Materials Science
IIT Indore

ACKNOWLEDGEMENT

I am highly indebted to my advisor, Dr. Eswara Prasad Korimilli whose support and guidance has driven me to do this work. His constant encouragement and constructive support enabled this work to achieve its present form.

I am thankful to Dr. Santosh Hosmani, DUGC-MEMS, Dr. P.M. Shirage, HOD-MEMS and the faculty of Department of Metallurgy Engineering and Materials Science for giving me the opportunity to carry out research work and providing the facilities.

I would like to express my sincere gratitude to Prof. U. Ramamurty, NTU, Singapore and Dr. Abhishek Chaturvedi, IISc, Bangalore for allowing access to nanoindentation facilities.

I am thankful to Dr. B. Praveen Kumar, ARDE, DRDO, Pune for providing the material for the experiment.

I would also thank Sophisticated Instrument Centre, IIT Indore for extending the SEM and XRD facilities.

I am thankful to all the members of the Mechanics of Materials Lab – Mr. Vaibhav Kathavate, Ms. Tulika Dixit, Mr. Abhinav Sharma, Mr. Chaitanya Vishwakarma and Mr. Janmejai Sharma.

Finally, I would like to thank my family for their affection, moral encouragement and constant support.

Harshal Sonagara
B.Tech. IV Year
Discipline of Metallurgy Engineering and Materials Science
IIT Indore

ABSTRACT

In the current scenario, piezoelectric materials find a unique role in widespread applications such as sensors, energy harvesting devices, ultrasonic transducers and MEMS. Piezoelectric material produces an electric field when it is subjected to external mechanical stress and vice versa. Although there has been significant research in the enhancement of functional characteristics and coupling coefficients of piezoelectric materials, the role of mechanical properties is still yet to be strongly investigated. Therefore, in current work, an attempt has been made to investigate the effect of composition, thermal treatment and domain configurations on the nanomechanical properties of a polycrystalline Lead-Zirconate-Titanate (PZT) piezoceramic material. The domain configurations are systematically varied by annealing the PZT samples slightly above and below their curie temperature, T_c. The X-ray diffraction patterns of as-received, sub- and above-T_c annealed PZT samples suggests the transformation in crystal structure from tetragonal (pristine) to cubic (annealed) crystal structure. Further, the piezo active property (d_{33}) measurements indicate the changes in the domain configuration due to the annealing treatment. The microstructural characterization of the PZT samples performed using Scanning Electron Microscopy (SEM) indicate that the annealing treatment has no major influence on the grain size. Further, Energy Dispersive Spectroscopy (EDS) studies are carried out in conjunction with SEM to confirm the chemical composition of the test materials. Piezoresponse Force Microscopy (PFM) is used for characterizing the local changes in the domain as a result of thermal treatment. The high contrast regions in PFM images demonstrate the localised domain wall configuration and piezoactive regions. Further, the nanomechanical properties (e.g. hardness, H and elastic modulus, E) are investigated using instrumented nanoindentation. The experimental results indicate that both H and E are observed to follow the following sequence: *Annealed* > *Sub-annealed* > *pristine*. These observations are correlated to the underlying microstructural changes taken place during the annealing process.

TABLE OF CONTENTS

LIST OF FIGURES

LIST OF TABLES

CHAPTER 1: INTRODUCTION

Piezoelectric materials are a special class of materials which exhibit direct coupling between mechanical and electrical field and vice-versa. In their actual practice, these materials generate the charge on the surface when subjected to external loading and/or deform mechanically by the action of direct electric field, first one is recognized as direct (or sensor) effect while later one happens to be the converse (or actuation) effect (Fig. 1). Owing to their high electromechanical coupling coefficient, dielectric constants and piezoelectric constants, piezoelectric materials are used in widespread applications such as sensors, actuators, SONAR, MEMS, NEMS, and energy harvesting devices [1-3].

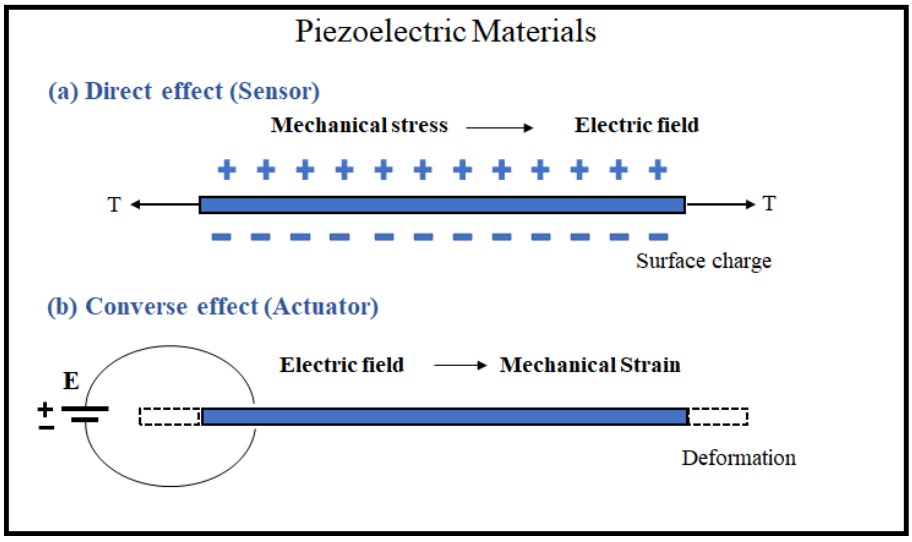

Figure 1. Direct and Converse Piezoelectric Effect

Often in their applications, piezoelectric material uses a ceramic made up of several oxides of various compounds such as lead (Pb), zirconate (Zr), Titanium (Ti), barium (B) and strontium (Sr). Among all the piezoelectric materials, perhaps, the most popular ones are conventionally used lead zirconate titanate (PZT), lead magnesium niobate-lead titanate (PMN-PT), barium titanate ($BaTiO_3$), and strontium titanate ($SrTiO_3$). As described earlier, piezoelectric ceramics (hereafter referred to as piezoceramics) is bulk of several perovskites having ABO_3 type crystals structure [4], typically composed of a

small, tetravalent metal ion placed inside a cage of larger divalent metal ions and oxygen atoms (Fig. 2).

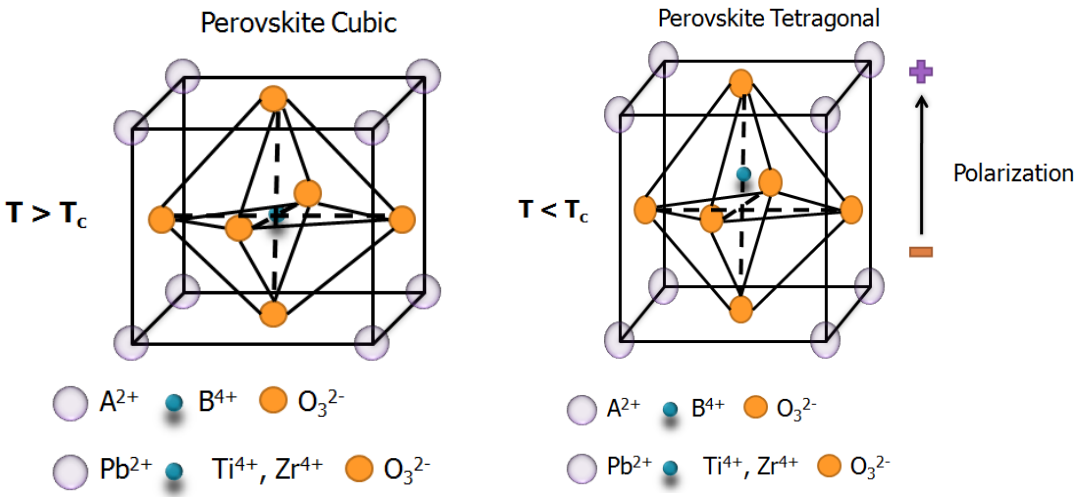

Figure 2. Crystalline structure of a piezoelectric ceramic (PZT), before and after polarization

Above certain critical temperature, known as the "*Curie temperature*, T_c", each perovskite crystal in the piezoceramic exhibits a simple cubic symmetry with zero polarization (piezoelectrically inactive phase- paraelectric). However, at temperatures par below the T_c, the crystal symmetry breaks down and the phase containing the distorted and asymmetric crystallites is often termed as ferroelectric phase (piezoelectrically active) [5]. The first scientific report on piezoelectric materials came into existence in the 1880s [6]. However, over the last three decades, there are voluminous studies performed focussing electrical characterization of these piezoceramics materials for their improved functional and structural characteristics using different techniques [7-11], perhaps, the most popular one is domain engineering. It is well estimated that the domains (Fig. 3), a local region formed within the grain due to directional alignment of dipoles may alter the structural and functional properties of these piezoceramics [12-14].

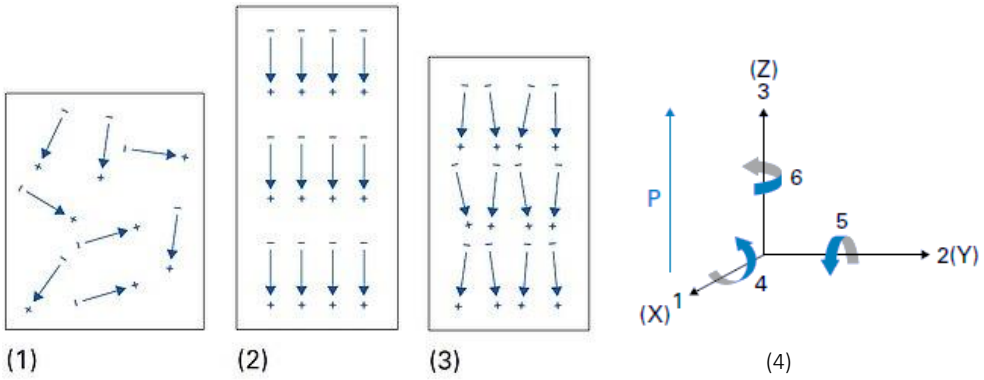

Figure 3. Schematic representation of the poling process in piezoceramic [15]. (1) Random orientation of polar domains prior to polarization (2) Polarization by an external electric field, the sample is elongated in the poling direction (3) Remnant polarization after the electric field is removed; the specimen is permanently elongated. (4) Orthogonal system to describe the properties of a polarized piezo ceramic. Axis 3 is the direction of polarization

Piezoceramics like PZT can be doped with other ions for enhancing its properties for specific applications. Although there are different types of piezoelectric ceramic materials available today, most can be placed into one of two general categories: “Hard” materials and “Soft” materials.

Hard piezoceramics are doped with acceptor dopants which cause anion (oxygen) vacancies in the crystal. In an undoped PZT, while sintering is done, some holes are formed due to evaporation of lead oxide. And on doping the ceramics with acceptor dopants like K^+ or $Fe^{3+,}$ space charges, i.e., the centres of positive and negative charges, increase dramatically which results in an internal electric field, E_s, in the grains of the material. This electric fields impede the movements of the domains and hence are responsible for inhibiting domain wall motion. Due to this, they are more difficult to polarize and depolarize. Curie Temperature of hard ceramics is generally above 300 ^oC [16]. They can resist high electric fields and temperatures and can withstand large mechanical stresses. Due to these properties of hard piezoceramics, they are suitable for high power applications like ultrasonic cleaning, welders or transducers. Equations (1)-(4) represent doping in PZT using Kröger–Vink notation. When PZT is doped by acceptor dopants, K^+ (replaces Pb^{2+}) and Fe^{3+} (replaces Ti^{4+}),

as shown in equation (1) and (2) respectively, to maintain electroneutrality, an oxygen vacancy is created.

$$K_2O \xrightarrow{PZT} 2K'_{Pb} + V_O^{\cdot\cdot} + O_o^{\mathrm{x}} \quad (1)$$

$$Fe_2O_3 \xrightarrow{PZT} 2Fe'_{Ti} + V_O^{\cdot\cdot} + 3O_o^{\mathrm{x}} \quad (2)$$

Soft piezoceramics are doped with donor dopants which causes cation (metal) vacancies in the crystal. These cation vacancies make the transfer of atoms easier as compared to the transfer in a perfect lattice. These ease of transfer makes the domain wall motion possible even at low electric fields or low mechanical stresses [17]. Soft ceramics generally have low Curie points below 300 ^{o}C. They produce wider signal bandwidths and larger displacements, as compared to hard ceramics, but they exhibit greater hysteresis and are more susceptible to depolarization or other deterioration. Because of these characteristics, soft ceramics are primarily used in high sensitivity applications rather than in power applications. When PZT is doped by donor dopants, La^{3+} (replaces Pb^{2+}) and Nb^{5+} (replaces Ti^{4+}), as shown in equation (3) and (4) respectively, to maintain electroneutrality, lead vacancy is created.

$$La_2O_3 \xrightarrow{PZT} 2La_{Pb}^{\cdot} + V_{Pb}'' + 2O_o^{\mathrm{x}} \quad (3)$$

$$Nb_2O_5 \xrightarrow{PZT} 2Nb_{Ti}^{\cdot} + V_{Pb}'' + 4O_o^{\mathrm{x}} \quad (4)$$

The ability to build new piezoelectric devices by tailoring material to a specific application resulted in a number of developments, and inventions such as powerful sonars, piezo ignition systems, sensitive hydrophones and ceramic phono cartridges.

In past, although an extensive critique regarding the electrical performance of these piezoceramics is presented [7-11], the mechanical performance of these piezoceramics is still a poorly understood phenomenon. This may be probably due to the lack of experimental techniques. But in the current scenario, it is possible to probe the mechanical properties of

piezoceramics using nanoindentation technique. Unlike microindentation, the loads in the nanoindentation process can be varied from few μN to mN while indenter displacement into the material can be observed up to a few nanometres. In current work, nanoindentation, which is a fast and accurate means for investigating nanomechanical properties, is used to measure localized nanomechanical properties such as elastic modulus and hardness of the material. However, the current work is intended to interpose the enhancement in mechanical properties of these piezoceramics for durable service life.

CHAPTER 2: LITERATURE REVIEW

2.1 Review of Research on Piezoceramic Materials

This section provides an insight into the past research work on domain engineering of piezoceramic materials. It also highlights various techniques adopted by researchers to enhance and tailor the properties of piezoceramic materials.

Xiaoping Li *et al.* [18**]** investigated the effect of transverse tensile stress on the electric-field induced domain reorientation. Properties under investigation were $I_{(002)}/I_{(200)}$, which represents the ratio of the volume of the c-domains to that of the a-domains on the PZT surface and $d_{31,\,domain}$ value, which denotes the part of d_{31} that is caused by domain reorientation. They reported that with transverse tensile stress of 75 MPa, $I_{(002)}/I_{(200)}$ increased with an upward curvature with the electric field, indicating that the stress enhanced the field-induced 90°-domain reorientation, and increased the effective piezoelectric coefficients at larger electric fields. At E=900 kV/m, the estimated $d_{31\,,domain}$ changed from (-200 x 10^{-12}) V/m at zero stress, to (-350 x 10^{-12}) V/m at 75 MPa. In addition, as $I_{(002)}/I_{(200)}$ is larger than 0.5 on the polished surface it indicates that the polishing resulted in a c-domain preference on the sample surface. However, it is not clear how polishing can bring about a c-domain preference.

Makino and Kamiya [19**]** did the experimental study on effects of dc electric field on mechanical properties of piezoelectric ceramics. They investigated mechanical properties such as hardness, flexural fatigue strength, flexural strength and toughness of PZT. They found that hardness and fracture toughness were not influenced by the dc electric field, whereas the flexural strength and the fatigue strength degraded with the absolute value of the electric field. Hardness and fracture toughness were not influenced by the dc electric field, whereas the flexural strength and the fatigue strength degraded with the absolute

value of the electric field. The main cause of strength degradation and fatigue acceleration in piezoelectric ceramics is estimated to be the microscopic internal stress which is generated at the grain boundary by the piezoelectric and domain switching deformations. They used Vicker's indentation test and 3-point flexural test for investigating mechanical properties.

W. Bai *et al.* [20**]** used Template Grain Growth (TGG) of BNT-BKT-BT ceramics using BaTiO3 anisotropic particles as a template to tailor the strain response behaviour under a low driving field. The strain response exhibited an increasing trend with the increasing grain orientation, and remarkably giant S_{max}/E_{max} of 800 pm/V was acquired under a relatively low electric field of 45 kV/cm in the optimized microstructure for textured BNT-BKT–1BT ceramics compared with the reported lead-free Bi-based perovskite ceramics. The achieved textured ceramics showed prominent electric field- and temperature-dependent strain characteristic featured by both a high room-temperature S_{max}/E_{max}. of 621 pm/V under a very low driving field of 35 kV/cm and an achievable large S_{max}/E_{max} of 531 pm/V with almost vanished hysteretic behaviour at high temperature. Gaint S_{max}/E_{max} ratio was achieved under the low driving field for <100> textured BNT-BKT-BT and also at high evaluated temperature. In addition, strain response was found to increase monotonously with an increase of grain orientation.

Kumar, Lonkar and Balasubramanian [21**]** studied quantification of phases, grain size and relative density of PNS-PZT samples. In addition, electromechanical properties like d33, g33, FoM were also investigated. The samples were sintered at 1170, 1220, 1270, 1320 ^{o}C for checking optimum sintering temperature. They used XRD, High-Resolution TEM, d33 measurement, FESEM, Capacitance measurement, Broad Band Dielectric Analyser and Selective Area Electron Diffraction (SAED) for the sample characterization. They found that optimum sintering temperature was 1220 ^{o}C which had (1) compact and uniform microstructure (2) composition close to

Morphotropic Phase Boundary of PZT with optimum tetragonality, which resulted in better electromechanical properties.

Kounga *et al.* [22**]** investigated the poling behaviour of PZT ceramic by measuring ferroelectric hysteresis, the longitudinal piezoelectric coefficient, and field-cooling poling experiments. They did Rietveld refinement of XRD data of sample at different temperatures. They reported that field cooling is an effective way to obtain high piezoelectric coefficients with a comparably low applied electrical field, but there is still an energy threshold that must be overcome by the electric field to reach a maximum value of the polarization and d33. It is possible that due to this compensation for depolarizing fields, a stable macroscopic polarization can be achieved at high temperatures even for low poling fields, eliminating the field threshold observed in our experiments. However, the time scale required for this effect to be observed was outside the scope of their investigation.

Park *et al.* [23**]** have carried research to study domain switching and to measure the mechanical properties of individual ferroelectric domains in a tetragonal $BaTiO_3$ single crystal. They performed nanoindentation studies in conjunction with Piezoresponse force microscopy for characterization. They found that nanoindentation can induce local domain switching. The *c* and *a* domains have similar hardness but different elastic moduli. They further confirmed the difference in elastic moduli by Nanoindentation modulus mapping on *c* and *a* domains. They used finite element modelling to simulate the plastic strain profiles and von Mises stress of the indentations on both *a* and *c* domains, which introduces a higher level of stress than the critical value for nucleation of domains.

2.2 Summary of Literature Review

A large number of studies have been performed on enhancing electrical properties of piezoceramic materials by domain engineering. Since no significant research has been done on enhancing mechanical properties of piezoelectric materials, the current work focuses on analysing influence of

ferroelectric domains on mechanical properties like nanohardness and elastic modulus.

CHAPTER 3: OBJECTIVES

The overreaching goal of this research study is to systematically investigate the role of microstructure, particularly the domain configurations, on the nanomechanical behaviour of piezoceramics. The following primary objectives have been framed to in-line with the aim of this study:

1. To evaluate the microstructure of as-received (or pristine) hard and soft piezoceramics.
2. To quantify the nature of phases and determine the crystal structure of piezoceramics using XRD analysis.
3. To systematically vary the domain configurations by annealing the samples below and above the curie temperature
4. To conduct nanoindentation studies on the PZT samples with different structural states and investigate the role of domain orientation on the nanomechanical properties e.g. hardness, elastic modulus and elastic recovery.
5. To characterize the effect of indentation load on hardness and elastic modulus.

CHAPTER 4: EXPERIMENTATIONS

4.1 Materials and Sample Preparation

The materials chosen for the current study are $Pb[Zr_{0.58}\ Ti_{0.42}]O_3$ (PZT-5J) and $Pb[Zr_{0.60}\ Ti_{0.40}]O_3$ (PZT-4H). The first one is conventionally recognised as soft PZT while later one as a hard PZT. The high purity oxides of lead - PbO (Sigma Aldrich), zirconium - ZrO_2 (Sigma Aldrich) and titanium - TiO_2 (Sigma Aldrich) were mixed in a stoichiometric ratio with 5 wt% polyvinyl alcohol (PVA) as a medium and milled for 24 hours at 900°C followed by subsequent granulation. This mixture is further uniaxially molded into disc size samples of diameter 21 mm and thickness 1.2 mm under 1 tonne/cm^2 pressure. These disc size specimens were sintered around 1100 ºC for 6 hours followed by subsequent mechanical polishing and later electroding by screen printing with silver paste. The as-prepared samples were poled along thickness direction in a silicon oil bath at a temperature around 60 °C under an applied electric field 30 kV/cm for 30 min. The objective of the current study is to investigate the role of domain configuration on nanomechanical properties of these piezoceramics through domain engineering, therefore, the as-received disc size specimens are subjected to a thermal treatment 30°C below and above the Curie temperature, T_c (T_c for PZT-5J is 300°C and that of PZT-4H is 350°C) with holding time of 2 hours. After thermal treatment, all the specimens were mechanically ground with SiC emery paper of various grit size and finally polished up to 0.1 μm diamond paste. The piezoelectric constant, d_{33} on all the classes of piezoceramics (i.e. pristine, subannealed and annealed) was determined along poling direction using a d_{33} meter (SINOCERA YE2730A) (Fig. 4).

Figure 4. d33 meter (SINOCERA YE2730A) [24]

4.2 Characterization Techniques

4.2.1 Metallurgical Characterization

The possible phases and crystal structure of thermally treated PZT-5J and PZT-4H samples were determined from X-ray diffraction (XRD) analysis performed using X-ray Diffractometer (Rigaku SmartLab) (Fig. 5) using Cu/K_{α} radiation (λ=1.5406 Å) in the range of diffraction angle 20°–80° with the step width of 0.02°. All the observed peaks were matched with the standards of Joint Commission on Powder Diffraction Standards (JCPDS) database and lattice parameters were determined from high-intensity peaks. The microstructural investigation and elemental chemical composition of all the classes of PZT samples were carried out using Scanning Electron Microscope (SEM) (JEOL JSM 7610 Plus) followed by energy dispersive spectroscopy (EDS) studies. Before performing SEM, all the samples were chemically and thermally etched to remove the unwanted micron level impurities and to separate the grains from grain boundaries. Etchants were prepared by diluting the solutions of HF and HNO_3 with Distilled Water (DW) as shown in Table 1.

Table 1. Recipes for etchant preparation and time of holding of samples in the etchants.

Sr. No.	Recipes for Etchant Preparation	Time of Holding
1	100 ml Distilled Water + 48 ml HF	2-3 minutes
2	100 ml Distilled Water + 40 ml HNO_3	3-4 minutes

Figure 5. X-ray Diffractometer (Rigaku SmartLab) [25]

4.2.2 Piezoresponse Force Microscopy (PFM)

Domain visualization and surface topography studies are conducted using Atomic Force Microscopy (AFM) of (Park Systems NX10) (Fig. 6) in PFM mode. An AC modulated voltage (V=5 Volts) was applied between a Ti/Ir conductive tip and a bottom electrode. The radius of curvature of the tip was 20 nm, having a resonance frequency 60 kHz and spring constant 2 N/m. AFM instrument was equipped with an external lock-in amplifier and a function generator which were used to apply the voltage on the sample surface for poling. Further, scanning of the surface is performed at slow scan speed 1 Hz with scan area 10 μm × 10 μm.

Figure 6. Atomic Force Microscopy (AFM) (Park Systems NX10) [26]

4.2.3 Nanoindentation Experiments

Figure 7. Hysitron TI Premier Nano indenter [27]

The quasistatic nanoindentation experiments were performed at room temperature with Berkovich three-sided pyramidal indenter using fully calibrated Hysitron TI Premier Nano indenter (Fig. 7) to obtain the nanomechanical properties of PZT-4H and PZT-5J samples. On each class of the samples, indents were made within the load range of 1 mN - 5 mN with an interval of 1 mN at a constant loading and unloading rate 0.5 mN/sec. Nanoindentation data is stochastic in nature and therefore, in present work 20 indents at each load were performed and only average values are reported to

make it statically representative. A typical indentation experiment consisted of four subsequent steps: approaching the surface, loading to peak load, holding the indenter for a dwell time of 2 seconds and finally unloading completely. The indenter is being held for the dwell period in order to relax the material before unloading. To avoid the strain field interactions within the grains beneath the indenter, the successive distance between two indents was kept at least 10 to 15 times the maximum penetration depth. After all the experiments, nanoindentation data was analysed for calculating the nanoindentation hardness and elastic modulus of the material using standard Oliver and Pharr method [28]. Below we present the equations for calculating nanoindentation hardness, *H* and elastic modulus, *E* [28].

Hardness, $$H = \frac{P_{max}}{A_c} \quad (5)$$

Elastic Modulus, $$E_s = (1 - {\nu_s}^2)\left[\frac{2\sqrt{A_c}}{S\sqrt{\pi}} - \frac{(1-{\nu_i}^2)}{E_i}\right]^{-1} \quad (6)$$

Here, *H*, *E* and ν are hardness, elastic modulus and Poisson's ratio respectively. The subscript *i* and *s* specifies the indenter and specimen under investigation respectively. Hardness and elastic modulus are computed from maximum indentation load P_{max}, contact area A_c and indentation stiffness *S*.

CHAPTER 5: RESULTS AND DISCUSSION

5.1 X-Ray Diffraction Analysis

Crystal structures of pristine, subannealed and annealed samples were obtained using X-ray diffraction patterns. Tetragonal crystal structure was observed for pristine and cubic crystal structure was observed for subannealed and annealed PZT samples. Fig. 8 (a) and Fig. 9 (a) shows the XRD patterns of PZT-4H and PZT-5J respectively. The XRD patterns of subannealed and annealed PZT samples are similar. The XRD pattern of pristine PZT-4H (Hard) shows sharp peaks at (111) and (022). This shows the preferential orientation of the grains in these directions [29]. The sharp peaks of subannealed and annealed PZT-4H samples were observed at (101). Similar behaviour is also observed for PZT-5J (Soft) samples. This indicates that annealing the samples has changed the orientation of crystals and might have caused the transformation of the crystal structure of PZT from tetragonal(pristine) to cubic (annealed) structure.

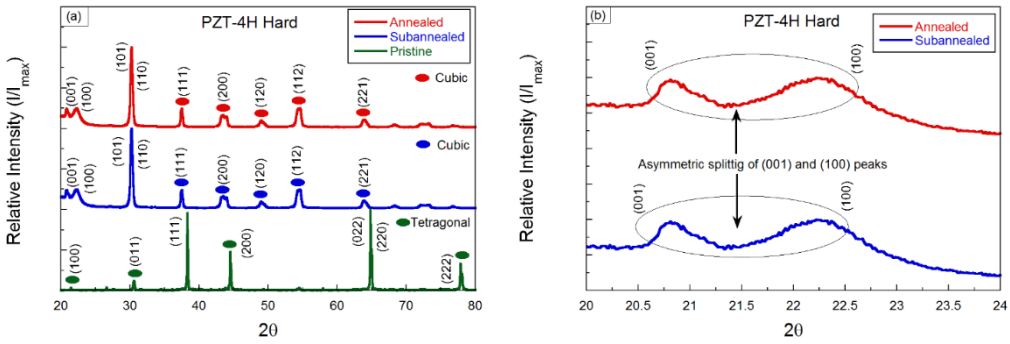

Figure 8. (a) X-ray diffraction pattern for pristine, subannealed and annealed PZT-4H (Hard) (b) Representation of peak splitting of subannealed and annealed PZT-4H (Hard).

It can be observed from the XRD pattern, that peak broadening has occurred in subannealed and annealed PZT samples in all the peaks after diffraction angle 45°. Peak broadening can occur when there are crystal defects in material or when there are insufficient number of planes for coherent diffraction [30]. The X-ray diffraction patterns of the subannealed and annealed samples of PZT-4H between diffraction angle 20° and 24° is magnified in Fig.8

(b). Asymmetric splitting of the (001) and (100) peaks is observed in Fig.8 (b) due to thermal treatment of the samples. Fig. 9 (b) shows the asymmetrical splitting of (200) and (002) peaks between diffraction angle 43° and 46° angle in subannealed and annealed samples of PZT-5J.

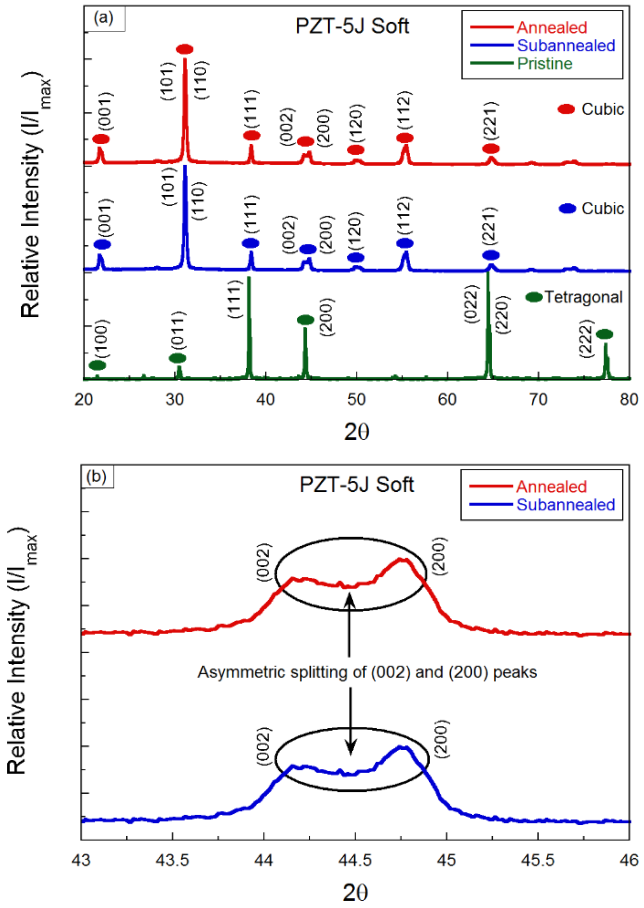

Figure 9. (a) X-ray diffraction pattern for pristine, subannealed and annealed PZT-5J (Soft) (b) Representation of peak splitting of subannealed and annealed PZT-5J (Soft).

5.2 Scanning Electron Microscopy (SEM) and Energy Dispersive Spectroscopy (EDS) Analysis

Microstructures of the samples were observed using a Scanning Electron Microscope. The representative SEM images of pristine, subannealed and annealed samples of PZT-4H and PZT-5J are shown in Fig. 10 and Fig. 11 respectively. Significant porosity can be observed in the pristine sample of PZT-5J as shown in Fig.11 (a). Impurities and unwanted substances are observed in

the SEM image of the pristine PZT-4H sample, shown in Fig. 10 (a). this may be due to the lesser etching time during chemical etching.

The average grain size of the PZT samples is determined using ImageJ software. The average grain size with standard deviation is shown in Table 2. At least 50 grains were taken for the measurements in order to represent the statistically representative measurements. Grain size-frequency distribution plot is displayed at the inset of each SEM image shown in Fig. 10 and Fig. 11.

Table 2. Average grain size with a standard deviation of PZT samples

Test material	**Pristine (µm)**	**Subannealed (µm)**	**Annealed (µm)**
PZT-4H (Hard)	1.33 ± 0.36	1.64 ± 0.56	2.30 ± 0.44
PZT-5J (Soft)	1.05 ± 0.27	1.37 ± 0.46	1.78 ± 0.39

The cubic crystals of annealed and subannealed PZT samples are bigger in size than the tetragonal crystals of pristine PZT samples. Fig. 10 and Fig. 11 shows that grains in annealed PZT samples are appearing to be more compact than pristine samples due to annealing treatment above the Curie temperature.

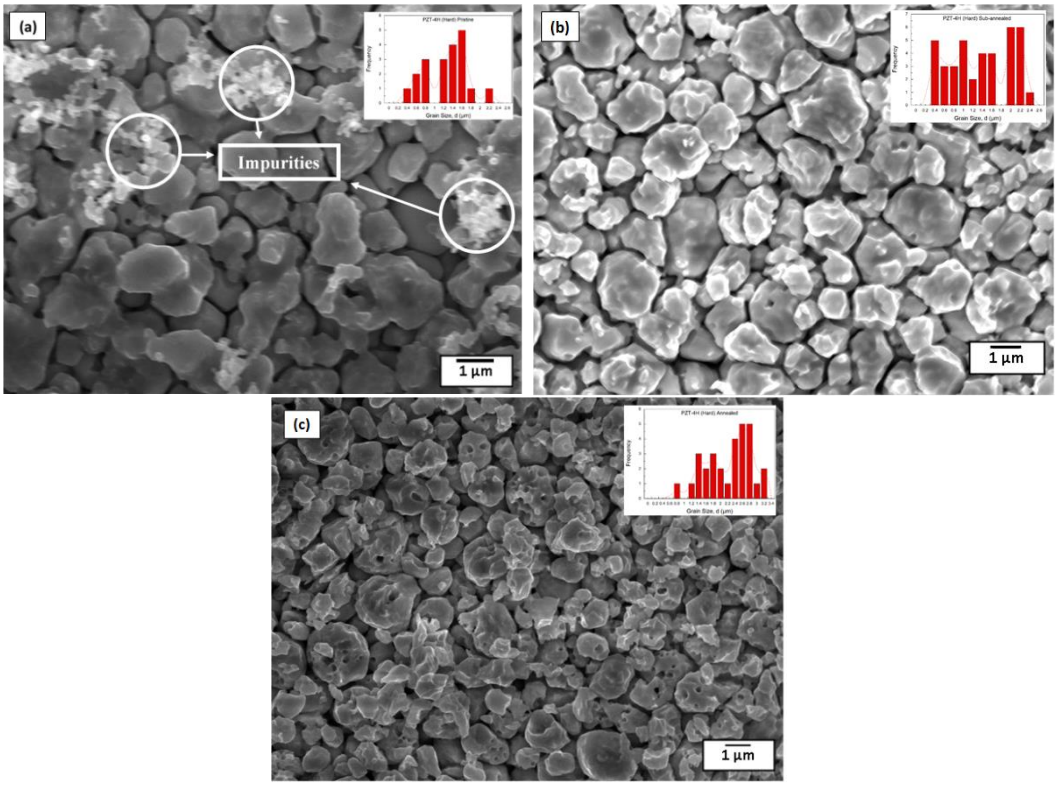

Figure 10. Scanning Electron Microscope images of (a) pristine, (b) subannealed and (c) annealed PZT-4H with corresponding grain size-frequency distribution plot shown in the inset.

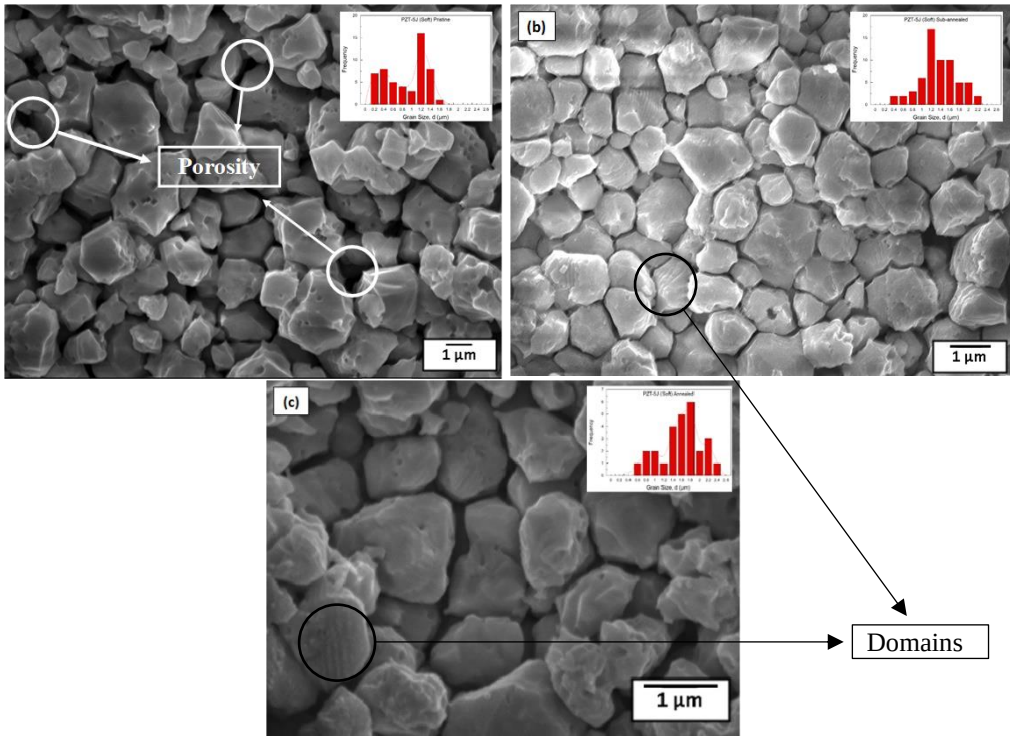

Figure 11. Scanning Electron Microscope images of (a) pristine, (b) subannealed and (c) annealed PZT- 5J (Soft) with corresponding grain size-frequency distribution plot shown in the inset

To determine the chemical composition of PZT piezoceramics, Energy dispersive spectroscopy (EDS) study was performed in conjunction with SEM. It can be seen from Fig. 12 and Fig. 13 that both the samples exhibited the presence of lead (Pb), zirconium (Zr), titanium (Ti) and oxygen (O). Among all the elements lead (Pb) is found to be a major constituent element in the test material.

The elemental compositions of the samples are shown in Table 3. Some additional elements such as carbon (C), silicon (Si) and gold (Au) are also detected in the EDS mapping of the classes of the test material. However, we only mentioned the major elements detected in the EDS studies.

Table 3. Weight percentage of major elements present in PZT-4H and PZT-5J

Elements	Weight % (PZT-4H)	Weight % (PZT-5J)
Pb	63.3	62.8
Zr	16.6	16.2
Ti	5.7	6.2
O	14.3	14.6

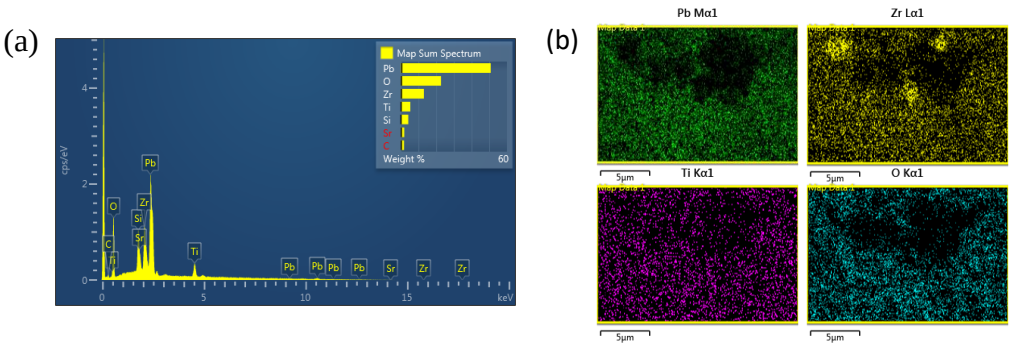

Figure 12. (a) Energy dispersive spectroscopy of Hard PZT on the scanning electron microscope (EDS-SEM). (b) Inset shows the EDS analysis area. EDS map showing detection of Pb (green), Zr (yellow), Ti (Purple), Oxygen (cyan).

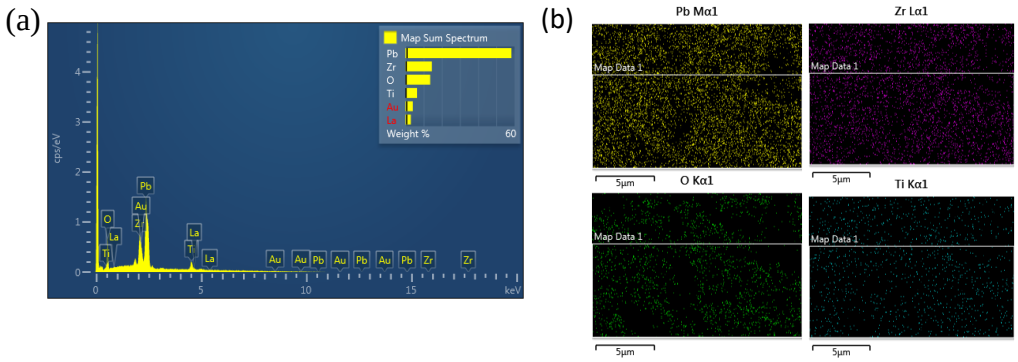

Figure 13. (a) Energy dispersive spectroscopy of Soft PZT on the scanning electron microscope (EDS-SEM). (b) Inset shows the EDS analysis area. EDS map showing detection of Pb (yellow) Zr (purple), Ti (cyan) and Oxygen (green).

5.3 d_{33} value measurement

Table 4. Piezoelectric coefficient, d33 values of PZT samples

Materials	Pristine	Subannealed	Annealed
PZT-4H (Hard)	315 pC/N	148 pC/N	0 pC/N
PZT-5J (Soft)	465 pC/N	220 pC/N	0 pC/N

Piezoactive nature of the sample was analysed by measuring the piezoelectric coefficient, d_{33} using d_{33} meter. The values of d_{33} (in pC/N) are reported in Table 4. The upper working temperature of piezoceramics is limited by their Curie temperature, so above that Curie temperature piezoceramics loses their piezoelectric properties. Similar trends are also observed in our present study. Due to the thermal treatment on the material, a phase transition occurs at the Curie temperature from the polar crystal structure (tetragonal) to the non-polar crystal structure (simple cubic). Cubic crystal is a symmetric crystal with no polar axis, because of this, its d_{33} value is found to be zero. The tetragonal crystal structure of pristine PZT is polar due to its asymmetry, shows piezoelectric effect and thus has a non-zero d_{33} value. Although the X-ray diffraction patterns of subannealed PZT-4H and PZT-5J suggest a shift in crystal structure from tetragonal to cubic, it is interesting to see the non-zero values of Piezoelectric coefficient (d_{33}). There might be the possibility of

incomplete transformation from tetragonal to cubic phase. However, this further needs detailed investigation using phase quantification studies from XRD data.

5.4 Piezoresponse Force Microscopy (PFM) Analysis

Fig. (14) to Fig. (19) shows the Piezoresponse Force Microscopy images of (10μm x 10μm) region of PZT-4H and PZT-5J samples. Each sample is scanned using conducting tip radius 20 nm and the representative PFM images are shown below. The bright spots on the surface show piezoactive regions. Domains are observed in some of the grains of pristine PZT samples. In these regions, the orientation of dipoles is such that the conductive tip is able to excite the deformation in the direction perpendicular to the surface [31]. It can be observed that pristine samples have more grains with piezoactive regions, on the other hand, annealed samples have few piezoactive regions.

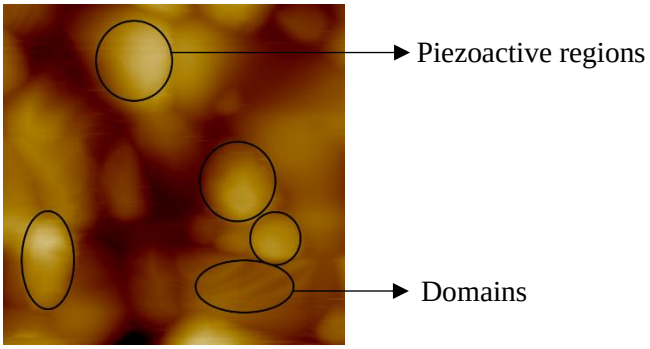

Figure 14. Representative PFM image of Pristine PZT-4H sample with scan area (10μm x 10μm)

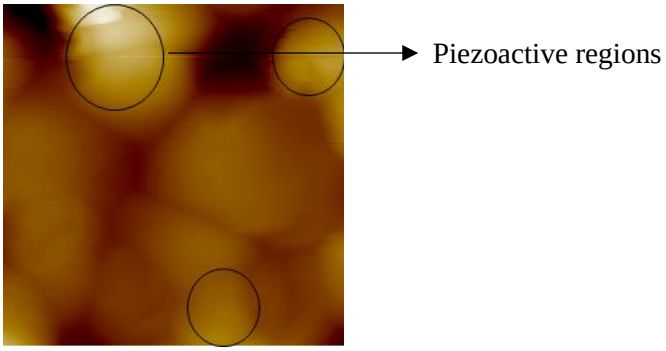

Figure 15. Representative PFM image of Subannealed PZT-4H with scan area (10μm x 10μm)

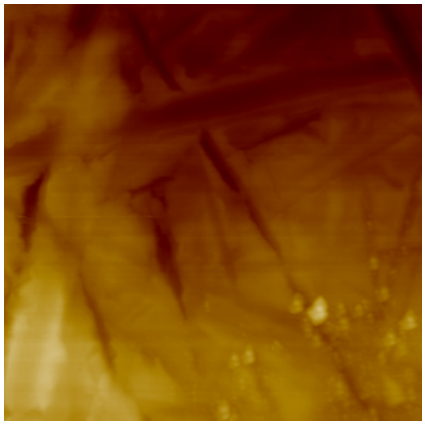

Figure 16. Representative PFM image of Annealed PZT-4H sample with scan area (10μm x 10μm)

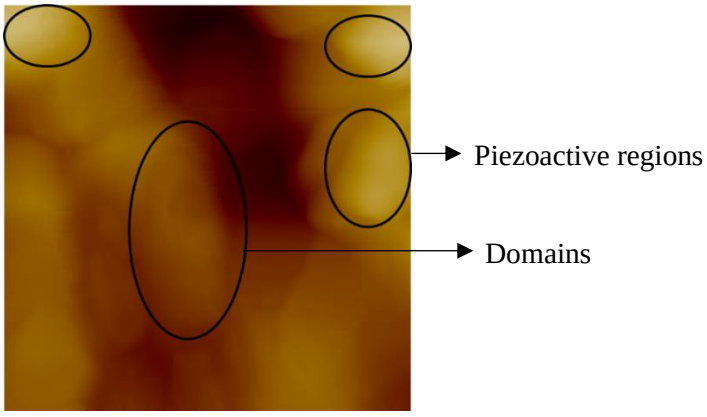

Figure 17. Representative PFM image of Pristine PZT-5J sample with scan area (10μm x 10μm)

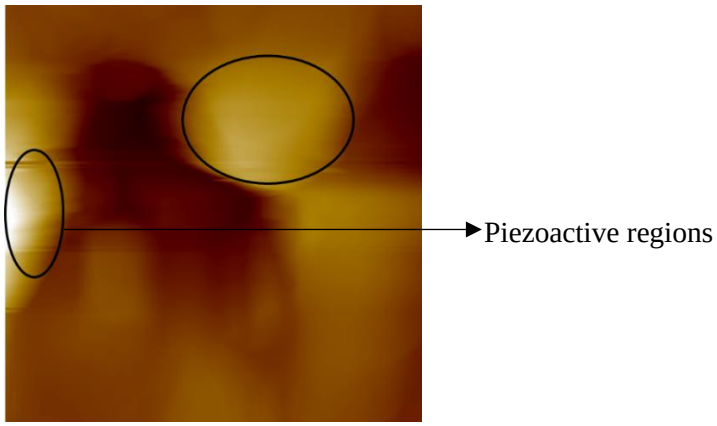

Figure 18. Representative PFM image of Subannealed PZT-5J with scan area (10μm x 10μm)

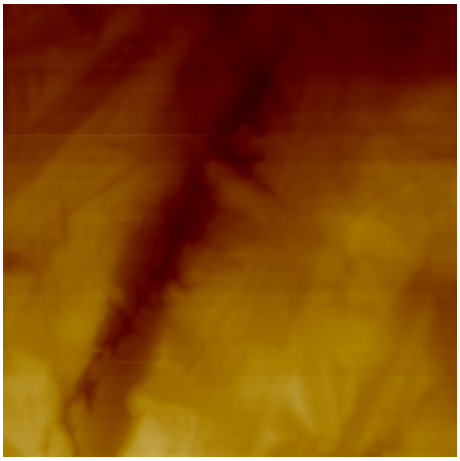

Figure 19. Representative PFM image of Annealed PZT-5J sample with scan area (10μm x 10μm)

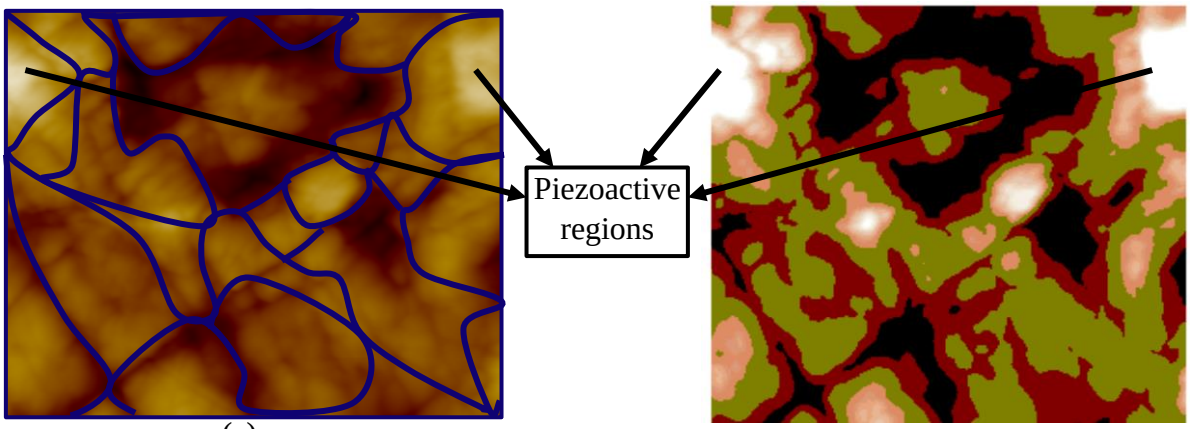

Figure 20. (a)Representative image of Piezoresponse Force Microscopy of PZT-4H sample with scan area (2.5μm x 2.5μm) and (b) its high contrast mapping.

Fig. 20 (a) shows even more magnified PFM image of PZT-4H with scan area (2.5μm x 2.5μm). The contour lines are separating the bright and dark regions in the scanning area. As the average grain size of our sample is 1.33 μm, it can be assumed that in our scanning area one or two grains are present, while there are more than 10 different piezoactive regions. So, from this, it can be inferred that multiple regions of different piezoactiveness are observed in a single grain which are called domains and the contours separating them are

domain walls. Fig. 20(b) is the high contrasted mapping of the representative PFM image.

5.5 Nanoindentation Analysis

5.5.1 Analysis of Load-Displacement curves

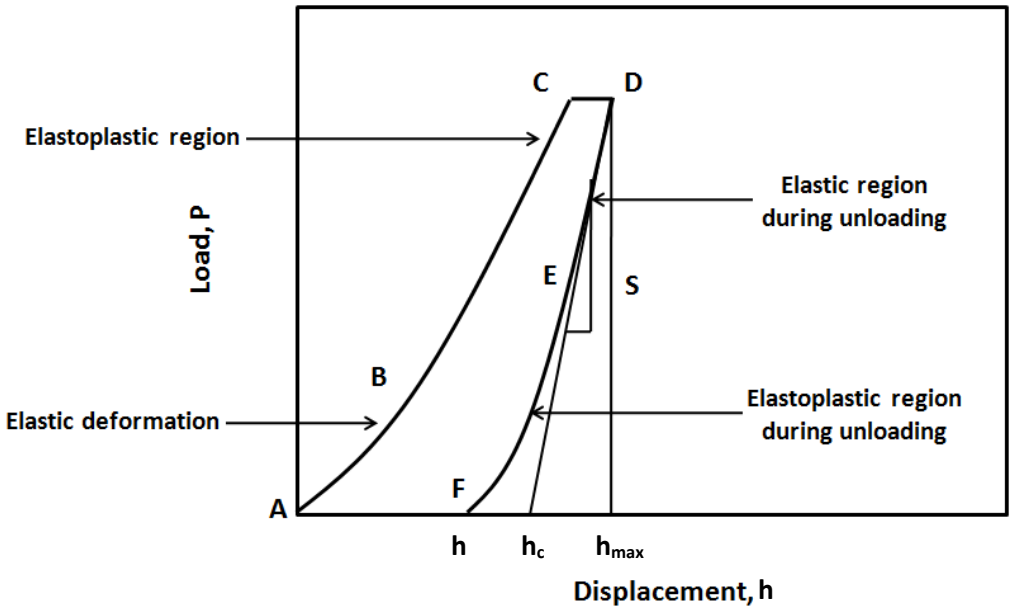

Figure 21. Load (P) vs Displacement (h) curves

According to Oliver and Pharr [28], the loading curve and the unloading curve can be represented by the equations (3) and (4) respectively,

Loading Curve, $P=\alpha h^m$ (7)

Unloading Curve, $P= \alpha(h-h_f)^m$ (8)

The two mechanical properties measured most frequently using load and depth sensing indentation techniques are the elastic modulus, E, and the hardness, H.

Hardness, $H = \frac{P_{max}}{A_c}$ (9)

Elastic Modulus, $E_s = (1 - \nu_s{}^2)\left[\frac{2\sqrt{A_c}}{S\sqrt{\pi}} - \frac{(1-\nu_i{}^2)}{E_i}\right]^{-1}$ (10)

Representative load-displacement curves for pristine, subannealed and annealed samples of PZT-4H and PZT-5J are shown.

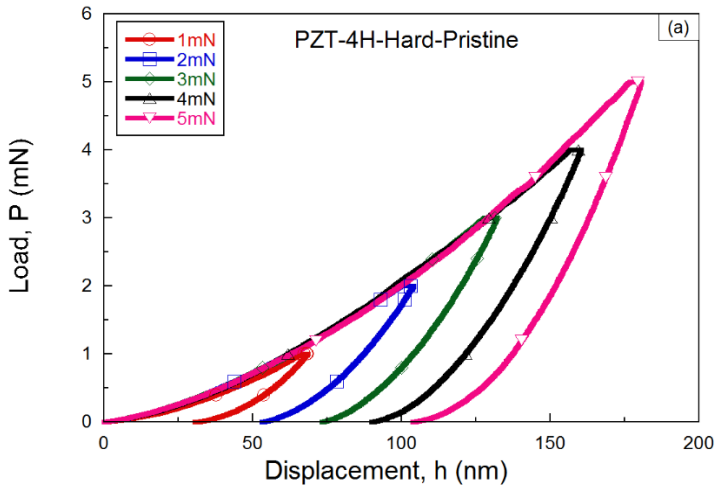

Figure 22. Representative Load vs Displacement curve for Pristine PZT-4H

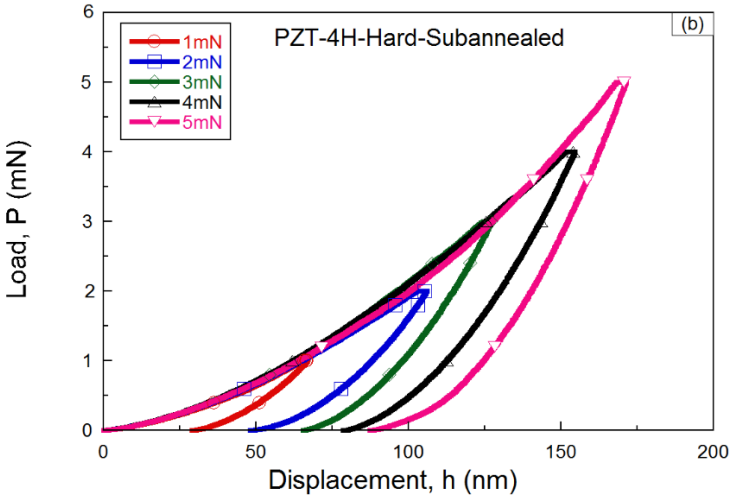

Figure 23. Representative Load vs Displacement curve for Subannealed PZT-4H

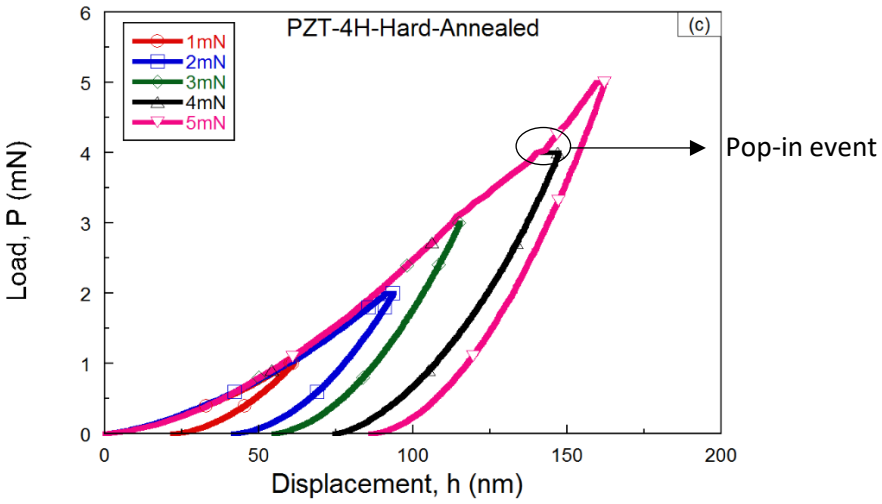

Figure 24. Representative Load-Displacement curve for Annealed PZT-4H

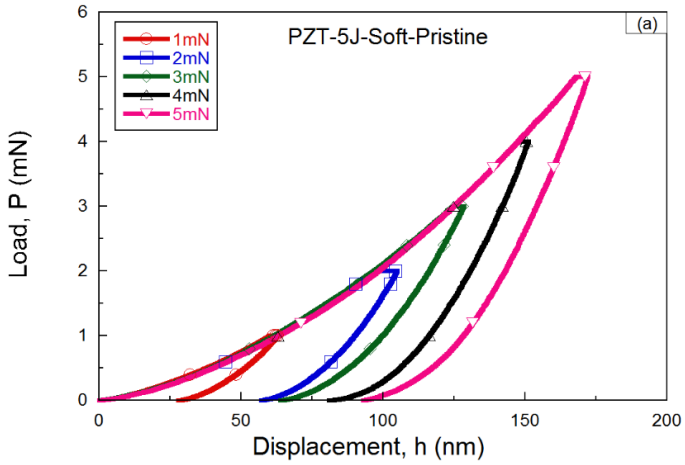

Figure 25. Representative Load-Displacement curve for Pristine PZT-5J

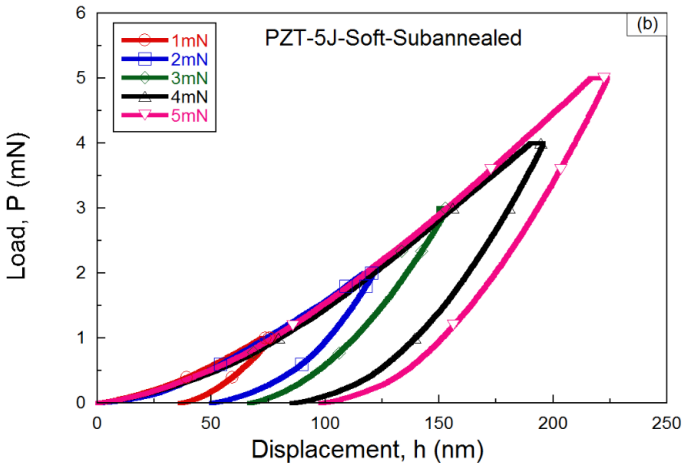

Figure 26. Representative Load-Displacement curve for Subannealed PZT-5J

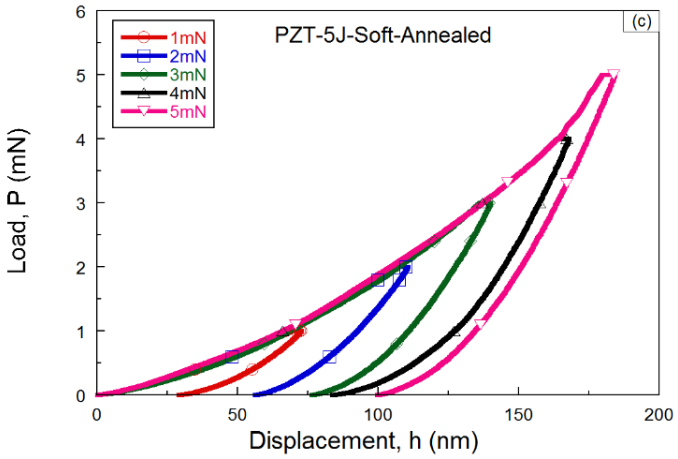

Figure 27. Representative Load-Displacement curve for Annealed PZT-5J

All the loading curves are fitted using power-law behaviour, $P=\alpha h^m$, as described in the literature [28] with the α and m values in the range of 1.5 as typically observed for Berkovich indentations.

A small pop-in can be seen in Fig. 24 Load vs Displacement curve of Subannealed PZT-4H during loading the sample at 5mN. A pop-in event is a sudden (load or displacement) burst during the loading of an indenter on a sample. If the nanoindentation experiment is load-controlled, a horizontal plateau is also observed on the load-displacement curve, when a pop-in occurs at the critical load and critical displacement. In the case of a displacement-controlled nanoindentation experiment, a vertical drop of the load is observed on the load-displacement curve. Such pop-ins in the loading curves are often attributed to the cracking of the material or pressure-induced phase transformation [32].

5.5.2 Hardness measurement

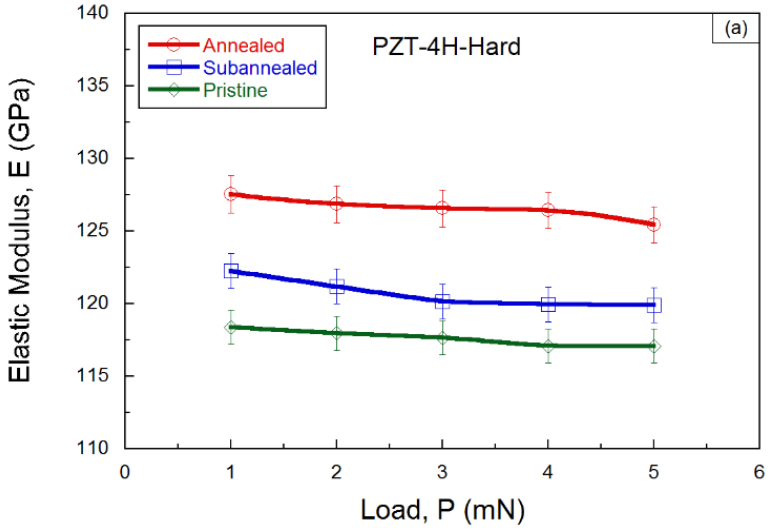

Figure 28. Elastic Modulus of PZT-4H at different loads

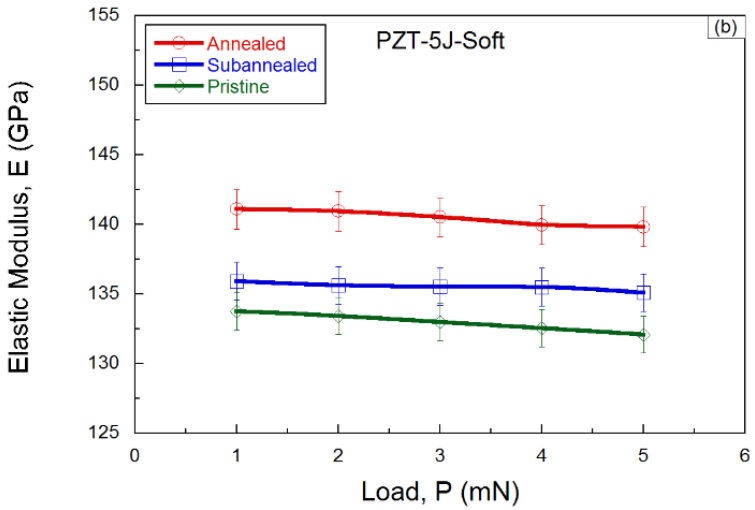

Figure 29. Elastic Modulus of PZT-5J at different loads

Table 5. Elastic Modulus (GPa) of PZT samples

	Annealed	Subannealed	Pristine
PZT-4H	125.46	119.90	117.09
PZT-5J	139.84	135.10	132.10

It can be observed that the elastic modulus of Annealed samples is highest for both the materials. There is no significant variation in elastic modulus with the change in load. However, Robinson *et al.* [33] have reported an increase in apparent elastic modulus of $BaTiO_3$ with decreasing contact radii of the indenter. They attributed this peculiar elastic size-effect to flexoelectricity, which is defined as a spontaneous electrical polarization in response to strain gradient. Flexoelectricity may also significantly affect polarization behaviour in ferroelectric systems [34].

5.5.3 Hardness measurement

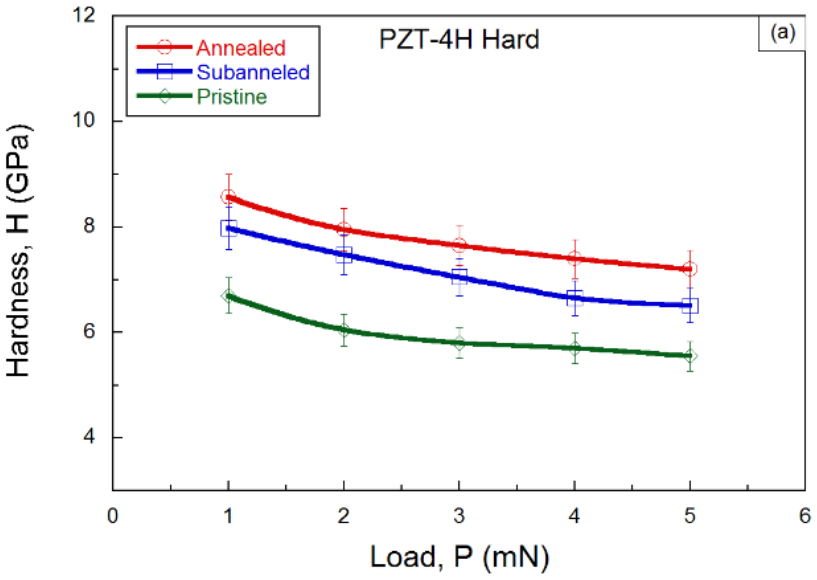

Figure 30. Hardness of PZT-4H at different loads

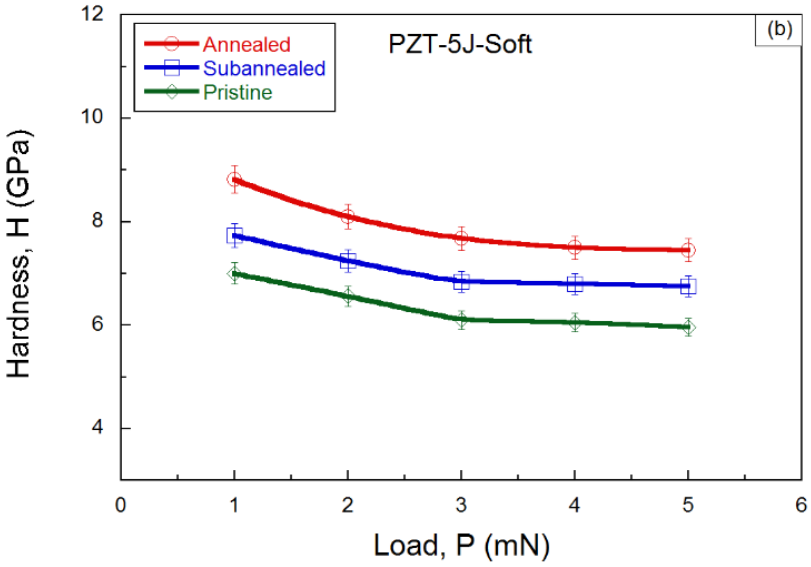

Figure 31. Hardness of PZT-5J at different loads

Table 6. Hardness (GPa) of PZT samples

	Annealed	Subannealed	Pristine
PZT-4H	7.20	6.51	5.55
PZT-5J	7.45	7.75	6.33

Hardness is also highest for the annealed samples of both the materials. However, unlike elastic modulus, there is significant variation (>5%) in the hardness of a sample with varying loads. Hardness is highest at 1 mN load and subsequently, it decreases with increasing loads. During the nanoindentation, a hard tip is pressed into the sample, and the variation of load versus the penetration depth is recorded. In the case of nanoindentation, the dependency of material hardness on the corresponding characteristic length is termed as the size effect. The underlying mechanism of the size effect during nanoindentation depends on material nature [35]. Sample size and shape can also influence the hardness value.

The mechanical properties of domains may influence the functionality of the ferroelectric devices. In addition, as the size of a device goes down to micro/ nano level, it consists of only a few domains. In this case, the mechanical properties of individual domains play a major role in the function of the device.

When an indentation size is comparable to the size of the sample, significant sample size effect can be observed. To determine the hardness accurately, nanoindentation must be done with *a/R* ratio (ratio of the radius of indent to the radius of specimen) less than 0.3, which is independent of shape and properties of materials [36]. As our samples were significantly larger and thicker than the indent, sample size effect has no influence in the hardness.

5.5.4 H/E Ratio

Table 7. H/E Ratio

	Annealed	Subannealed	Pristine
PZT-4H	0.0613	0.0591	0.0507
PZT-5J	0.0563	0.0522	0.0476

The ratio of Young's modulus, E, and the hardness, H, is an important parameter which has been frequently used in materials science to evaluate the brittleness and to determine the toughness by indentation. There have been several studies concerning the determination of H/E ratio from indentation tests [37,38]. The elastic recovery during the indentation is related to the ration *H/E*. According to the model proposed by Peng *et al.* [37], elastic recovery decreases with the *H/E* ratio.

It is evident from the table that the pristine samples show a greater elastic recovery than the annealed samples. The reason for this behaviour is attributed to the differences in domain orientations and the elasticity associated with them. In the case of pristine samples, upon unloading the domains would want to realign in the poling direction, while in the annealed sample due to the lack of domain ordering such recovery is not observed [38].

CHAPTER 6: CONCLUSIONS AND SCOPE FOR FUTURE WORK

6.1 Conclusions

In this study, the nanomechanical properties of two kinds of piezoelectric materials namely, PZT-4H and PZT-5J having different domain configurations are investigated. The following conclusions are drawn from this experimental study.

- The X-ray diffraction patterns of PZT samples reveals that annealing has caused a transformation in crystal structure from tetragonal (pristine) to cubic (annealed).
- Despite their similarity in the crystal structure, the subannealed samples exhibit higher d_{33} compared to the annealed samples ($d_{33} \sim 0$) suggesting that the domains are not completely randomized due to sub-T_c annealing.
- The surface morphology using Scanning Electron Microscopy (SEM) studies reveals that there are slight differences in the average grain size. These differences may have been introduced during the sintering process as the annealing temperatures used in this study are well below their sintering temperatures.
- The high and low contrast regions in Piezoresponse Force Microscope (PFM) images clearly distinguish the regions of high and low domain activities. These regions can be easily observed in the case of pristine samples than the sub- and above-T_c annealed samples.
- The hardness, H, contrary to the d33 measurements, indicates that annealed samples are harder than the subannealed and pristine samples. The possible reasons for this could be attributed to the changes taking place in the domain configuration during thermal treatment.
- Further, the H is observed to be decreasing with indentation load (for all the cases) suggesting that the PZT materials normally exhibit indentation size effect (ISE),
- Similar to the H, the elastic modulus, E of the annealed samples is highest for annealed samples.

6.2 Future Scope

The research can be extended to achieve a better understanding of the influence of domains on the properties of piezoceramics.

- To further analyse the variation in properties with thermal treatments, samples should be subjected to thermal treatment at temperatures $0.4T_c$, $0.6\ T_c$, $0.8\ T_c$, T_c and $1.2\ T_c$.
- The role of annealing time on d_{33} and H has to be ascertained.
- The role of strain gradient on the ISE and domain configurations can be studied using interface indentation experiments.
- The maximum loads in the current study are limited to 5 mN due to the limitations in the load cell. What happens to the H at high indentation loads is an interesting aspect to study.
- Also, at high loads, these ceramics (due to their brittle nature) tend to fracture and it is possible to measure the indentation fracture toughness from the morphology of the cracks. The role of domains on the indentation fracture toughness can be investigated.

REFERENCES

[1] Li, H., Tian, C. and Deng, Z.D.: *"Energy harvesting from low frequency applications using piezoelectric materials."* **Applied physics reviews**, 1(4), **2014**, p.041301.

[2] J. G. Gualtieri, J. A. Kosinski and A. Ballato: *"Piezoelectric materials for acoustic wave applications"* **IEEE Transactions on Ultrasonics, Ferroelectrics, and Frequency Control**, vol. 41, no. 1, **1994**, pp. 53-59.

[3] Manbachi, A., & Cobbold, R. S. C.: *"Development and Application of Piezoelectric Materials for Ultrasound Generation and Detection."* **Ultrasound,** *19*(4), **2011**., 187–196.

[4] Eman Abdul Rahman Assirey: *"Perovskite synthesis, properties and their related biochemical and industrial application",* **Saudi Pharmaceutical Journal**, Volume 27, Issue 6, **2019**, Pages 817-829.

[5] A.L. Kholkin, N.A. Pertsev, A.V. Goltsev: *"Piezoelectricity and Crystal Symmetry",* **Springer**, Chapter 2, 2008, Pg. 21.

[6] Curie, Jacques and Curie, Pierre: *"Development, via compression, of electric polarization in hemihedral crystals with inclined faces,"* **Bulletin de la Societe de Minerologique de France**, 3, **1880**, p. 90-93.

[7] Eitel, R.E., Shrout, T.R. and Randall, C.A.: *"Tailoring properties and performance of (1-x) $BiScO_3$–$xPbTiO_3$ based piezoceramics by lanthanum substitution."* **Japanese journal of applied physics**, *43*(12R), **2004**, p.8146.

[8] Zhang, S., Xia, R.U., Shrout, T.R., Zang, G. and Wang, J.: *"Characterization of lead free ($K_{0.5}$ $Na_{0.5}$)NbO_3–$LiSbO_3$ piezoceramic."* **Solid State Communications**, *141*(12), **2007**, pp.675-679

[9] Zhu, M., Liu, L., Hou, Y., Wang, H. and Yan, H.: *"Microstructure and electrical properties of MnO-doped ($Na_{0.5}$ $Bi_{0.5}$)$_{0.92}Ba_{0.08}$ TiO_3 lead-free piezoceramics."* **Journal of the American Ceramic Society**, *90*(1), **2007**, pp.120-124.

[10] Rubio-Marcos, F., Romero, J.J., Navarro-Rojero, M.G. and Fernandez, J.F.: *"Effect of ZnO on the structure, microstructure and electrical properties of KNN-modified piezoceramics."* **Journal of the European Ceramic Society**, *29*(14), **2009**, pp.3045-3052.

[11] Yoshii, K., Hiruma, Y., Nagata, H. and Takenaka, T.: *"Electrical properties and depolarization temperature of ($Bi_{1/2}Na_{1/2}$)TiO_3 – ($Bi_{1/2}K_{1/2}$) TiO_3 lead-free piezoelectric ceramics."* **Japanese journal of applied physics**, *45*(5S), **2009**, p.4493.

[12] Vendrell, X., García, J.E., Bril, X., Ochoa, D.A., Mestres, L. and Dezanneau, G.: "*Improving the functional properties of ($K_{0.5}$ $Na_{0.5}$) NbO_3 piezoceramics by acceptor doping*." **Journal of the European Ceramic Society**, *35*(1), **2015**, pp.125-130.

[13] Hao, J., Bai, W., Li, W. and Zhai, J.: *"Correlation Between the Microstructure and Electrical Properties in High-Performance ($Ba_{0.85}$ $Ca_{0.15}$)($Zr_{0.1}$ $Ti_{0.9}$)O_3 Lead-Free Piezoelectric Ceramics."*, **Journal of the American Ceramic Society**, *95*(6), **2012**, pp.1998-2006.

[14] Zuo, R., Rödel, J., Chen, R. and Li, L.: *"Sintering and electrical properties of lead-free $NaO.5KO.5NbO_3$ piezoelectric ceramics."* **Journal of the American Ceramic Society**, *89*(6), 2006, pp.2010-2015.

[15] "*Piezoelectric Ceramic Products: Fundamentals, Characteristics and Applications*", **PI Ceramic.**

[16] Web reference: "*americanpiezo.com/piezo-theory/ceramics.html*"

[17] Hammer, M., Monty, C., Endriss, A. and Hoffmann, M.J.: "*Correlation between surface texture and chemical composition in undoped, hard, and soft piezoelectric PZT ceramics."* **Journal of the American Ceramic Society**, *81*(3), **1998**, pp.721-724.

[18] Li, X., Shih, W.Y., Vartuli, J.S., Milius, D.L., Aksay, I.A. and Shih, W.H.: *"Effect of a Transverse Tensile Stress on the Electric-Field-Induced Domain Reorientation in Soft PZT: In Situ XRD Study."* **Journal of the American Ceramic Society**, *85*(4), **2002**, pp.844-850.

[19] Makino, H. and Kamiya, N.: *"Effects of dc electric field on mechanical properties of piezoelectric ceramics."* **Japanese journal of applied physics**, *33*(9S), **1994**, p.5323.

[20] Bai, W., Chen, D., Zheng, P., Zhang, J., Shen, B., Zhai, J. and Ji, Z.: *"Low electric field-driven giant strain response in < 001> textured BNT-based lead-free piezoelectric materials."* **Journal of materials science**, *52*(6), **2017**, pp.3169-3178.

[21] Kumar, H.H., Lonkar, C.M. and Balasubramanian, K.: "*Influence of microstructure on electromechanical properties of nano-crystalline La-$Pb(Ni_{1/3}Sb_{2/3})$-$PbZrTiO_3$ ferroelectric ceramics."* **Applied Physics A**, *123*(10), **2017**, p.615.

[22] Kounga, A.B., Granzow, T., Aulbach, E., Hinterstein, M. and Rödel, J.: *"High-temperature poling of ferroelectrics."* **Journal of Applied Physics**, *104*(2), **2008**, p.024116.

[23] Park, Y.B., Dicken, M.J., Xu, Z.H. and Li, X.: *"Nanoindentation of the a and c domains in a tetragonal $BaTiO_3$ single crystal."* **Journal of Applied Physics**, 102(8), **2007,** p.083507.

[24] Web reference: *americanpiezo.com/standard-products/d33-meter.html*

[25] Web reference: *rigaku.com/en/products/xrd/smartlab*

[26] Web reference: *parksystems.com/index.php/products/small-sample-afm/park-nx10/overview*

[27] Web reference: *bruker.com/products/surface-and-dimensional-analysis/nanomechanical-test-instruments/landing-pages/hysitron-nanoindenters.html*

[28] Oliver, W.C. and Pharr, G.M.: "*An improved technique for determining hardness and elastic modulus using load and displacement sensing indentation experiments."* **Journal of materials research**, *7*(6), **2004**, pp.1564-1583.

[29] Cinzia Giannini, Massimo Ladisa, Davide Altamura, Dritan Siliqi, Teresa Sibillano, Liberato De Caro; "*X-ray Diffraction: A Powerful Technique for the Multiple-Length-Scale Structural Analysis of Nanomaterials*", **MDPI**, **2016**.

[30] "*X-Ray Diffraction Line Broadening*", **Journal of Research of the National Institute of Standards and Technology,** Volume 98, Number 3, **1993**, Pg. 323-324.

[31] McGilly, L., Byrne, D., Harnagea, C., Schilling, A. and Gregg, J.M.: "*Imaging domains in $BaTiO_3$ single crystal nanostructures: comparing information from transmission electron microscopy and piezo-force microscopy."* **Journal of materials science**, *44*(19), **2009**, pp.5197-5204.

[32] Jian, S.R., Chen, G.J. and Juang, J.Y.: "*Nanoindentation-induced phase transformation in (1 1 0)-oriented Si single-crystals."* **Current Opinion in Solid State and Materials Science**, *14*(3-4), **2010**, pp.69-74.

[33] C. R. Robinson, K. W. White, and P. Sharma: "*Elucidating the mechanism for indentation size-effect in dielectrics."* **Applied Physics Letters**, 101(12):122901, **2012**

[34] Ma W, Cross LE.: "*Flexoelectric effect in ceramic lead zirconate titanate."* **Applied Physics Letters.**,86(7):072905, **2005**.

[35] Voyiadjis, G.Z. and Yaghoobi, M.: "*Review of nanoindentation size effect: Experiments and atomistic simulation."* **Crystals**, *7*(10), **2017**, p.321.

[36] Xu, Z.H. and Li, X.: "*Sample size effect on nanoindentation of micro-nanostructures."*, **Acta materialia**, *54*(6), **2006**, pp.1699-1703.

[37] Peng, Z., Gong, J. and Miao, H.: *"On the description of indentation size effect in hardness testing for ceramics: Analysis of the nanoindentation data*.", **Journal of the European Ceramic Society**, *24*(8), **2004**, pp.2193-2201.

[38] Kathavate, V. & K., E. Prasad & Kumar, B. & Roy Choudhury, Palash & Singh, Indrasen.: *"Nanoindentation Response of PZT and NKN-NT Piezoceramics.",* **Journal of Coupled Systems and Multiscale Dynamics**., 6.10, **2019**.